| | |
|---|---|
| Title | Convergence of low-frequency EFIE-based systems with weighted right-hand-side effect |
| Author(s) | LIU, Q; Sun, S; Chew, WC |
| Citation | IEEE Transactions on Antennas and Propagation, 2014, v. 62, p. 5108-5116 |
| Issued Date | 2014 |
| URL | http://hdl.handle.net/10722/217022 |
| Rights | Creative Commons: Attribution 3.0 Hong Kong License |

# Convergence of Low-Frequency EFIE-Based Systems With Weighted Right-Hand-Side Effect

Qin S. Liu, *Student Member, IEEE*, Sheng Sun, *Senior Member, IEEE*, and Weng Cho Chew, *Fellow, IEEE*

***Abstract*—This paper addresses the convergence of the electric-field integral equation (EFIE)-based matrix systems with the right-hand-side effect. The role of the right-hand-side excitation in determining the convergence rate of the iterative solvers is found to be important or even crucial at low frequencies. The weighted contributions from different singular vectors are decided by not only the corresponding singular values but also the right-hand side. Based on this understanding, we investigate the low-frequency stabilized form of both EFIE and Calderón multiplicative preconditioner EFIE (CMP-EFIE) on capacitive problems. For the parallel-plate capacitor excited by the delta-gap source, the singular vectors with small singular values cannot be excited, and the charge currents on the capacitive surface dominate. Thus, the stability of the EFIE-based system can be achieved at low frequencies. Detailed spectral analysis and convergent results are carried out in order to capture the physical nature of the problems.**

***Index Terms*—Low-frequency stability, perturbation method, right-hand-side effects, singular vectors, spectrum analysis.**

## I. Introduction

BESIDES the typical factors like the condition number and eigenvalue spectrum, the role of the right-hand-side excitation in determining the speed of convergence of an iterative solver is also found to be important or even crucial under some situations, such as antenna, circuit, or packaging problems, which are usually excited by current or voltage sources. Maxwell's equations have highly predictive power over a wide range of length scales, from the subatomic to intergalactic length scales, only if Maxwell's equations are solved correctly. Disparate sizes in geometrical models induce both low-frequency circuit physics and mid-frequency wave physics, resulting in ill-conditioned matrix equations. When the method of moments (MoM) is employed to solve surface integral equations in order to model electromagnetic problems, both electrical-field integral equation (EFIE) and magnetic-field integral equation (MFIE) are extensively used. Analysis for the system stability of EFIE and MFIE focuses on the conditioning analysis and eigenvalue spectrum analysis. MFIE is thought to be well conditioned because of its diagonal-dominant property. Unfortunately, many real physics problems cannot be formulated by MFIE since it is less accurate [1], [2] and is not applicable to open surfaces [3]. So we still need to work with the ill-conditioned EFIE. EFIE is known to become ill-conditioned at low frequencies since it suffers from the low-frequency breakdown problem. Thus, it is important to investigate the convergence phenomenon of the EFIE-based systems.

The eigenvalue spectrum and the condition number are two key factors that are usually thought to influence the iteration convergence of the MoM matrix system. In matrix analysis theory, the small condition number of the matrix usually indicates a well-conditioned system, and the clustering of the eigenvalues at a finite number that is away from zero or a smaller-than-one spectral radius will usually ensure the stable convergence of the matrix system. It was stated in [4] that the eigenvalues of the system matrix and the number of corresponding eigenvectors required to represent the right side of the equation determines the convergence rate of the iterative solution algorithms, and the increasing density of discretization, which brings the existence of the increasing high-order modes, will lead to the ill condition of the EFIE system matrix [5]. So far, several remedies to the EFIE low-frequency breakdown have been proposed, such as loop-tree/loop-star decomposition [6]–[8] or the augmented EFIE (A-EFIE) method [9], which contributes to improving the conditioning of the impedance matrix. Also there are methods which focus on obtaining a stable spectral property of the system matrix. It is investigated in [10] that the properties of the basis functions employed have direct influence on the eigenvalue spectrum of the resulting MoM matrix and the eigenvalues cluster around one after regularization by employing the multiresolution (MR) basis function, which brings a good convergence behavior similar to the second-kind integral equation. The success of the recent proposed Calderón multiplicative preconditioned EFIE (CMP-EFIE) method [5], [11], [12] also benefits from the preconditioning that has made the original EFIE into a second-kind Fredholm integral equation operator, and the use of the Chen–Wilton–Buffa–Christiansen (CWBC) basis function makes the Calderón preconditioner into a multiplicative form (CMP-EFIE) [13], which also avoids the singularity of the Gram matrix and some complicated operator projection manipulations. However, the CMP-EFIE method still breaks down at low frequencies because the analytical condition $\mathcal{T}_h^2 = 0$ cannot be guaranteed after discretization. The most common way to remedy the breakdown problem is to apply loop-star decomposition [14], [15], which, however, will lose

Manuscript received September 27, 2013; revised May 02, 2014; accepted July 18, 2014. Date of publication July 22, 2014; date of current version October 02, 2014. This work was supported in part by the Research Grants Council of Hong Kong (GRF 716112, 716713), in part by the University Grants Council of Hong Kong (Contract No. AoE/P-04/08) and Seed Funding (201111159201 and 201211159076). W. C. Chew is funded by NSF CCF Award 1218552 and SRC Task 2347.001. (*Corresponding author: S. Sun*.)

Q. S. Liu and S. Sun are with the Department of Electrical and Electronic Engineering, The University of Hong Kong, Hong Kong, China (e-mail: sunsheng@ieee.org).

W. C. Chew is with the Department of Electrical and Computer Engineering, University of Illinois at Urbana-Champaign, Urbana, IL 61801 USA.

Color versions of one or more of the figures in this paper are available online at http://ieeexplore.ieee.org.

Digital Object Identifier 10.1109/TAP.2014.2341696

the diagonal-dominant property for the matrix. As an extension, a basis-free loop-star decomposition is proposed [16]. The new equation is applicable to scattering, inductive, and capacitive problems, immune from both low-frequency and discretization breakdown. Another more explicit way is to manually remove the square of the hypersingular term ($\mathcal{T}_h^2$) [17] so that the remaining three terms ($\mathcal{T}_s^2 + \mathcal{T}_s\mathcal{T}_h + \mathcal{T}_h\mathcal{T}_s$) are stable at low frequencies. Unfortunately, although stable at low frequencies, MFIE, A-EFIE, and CMP-EFIE all suffer from the low-frequency inaccuracy problem for the solved currents. As a remedy, the perturbation method has been applied to capture the accurate currents at different frequency orders [1], [18]–[20].

In this paper, the right-hand-side effect is taken into consideration when we investigate the convergence phenomenon of the EFIE-based matrix systems dealing with capacitive problems. Indeed, EFIE, which is known to have low-frequency breakdown, is shown to be stable at low frequencies when dealing with symmetric capacitive structures. The same could also be true of CMP-EFIE after removing the incorrect frequency-dependent terms. Detailed spectral analysis for both EFIE and CMP-EFIE systems is presented and discussed in the following sections. It is then pointed out that the right-hand-side effect is the key issue that is responsible to the convergence of the system. Under the delta-gap excitation, the singular vectors with small singular values, which will cause the slow convergence of the iterative system, cannot be excited. Also, in order to stabilize the CMP-EFIE system, the induction term with very small eigenvalues is removable at low frequencies when the charge term dominates. Thus, we can get the low-frequency stabilized form of EFIE and CMP-EFIE for capacitive problems.

The contributions of this paper are threefold: 1) it presents the theory of analyzing the right-hand-side effect in studying the convergence of an iterative system; 2) it investigates the weighted right-hand-side effect of the EFIE-based systems in solving capacitive problems, and thus the corresponding stabilized forms of EFIE and CMP-EFIE are studied; and 3) it verifies the accuracy of the simplified CMP-EFIE in solving the low-frequency capacitive problem using the right-hand-side effect analysis.

The paper is organized as follows. In Section II-A, first we define the physical problem and bring out the convergence issue. Then, Section II-B provides a mathematical manipulation of the right-hand-side effect in the iterative process; following in Section II-C is the detailed right-hand-side effect analysis of EFIE on capacitive problems at low frequencies, and also a stabilized form of EFIE is studied. Next, the simplified CMP-EFIE is analyzed in Section III-A. In addition, through the perturbation analysis in Section III-B, the convergence and accuracy of simplified CMP-EFIE is verified. Finally, Section IV presents more numerical results with asymmetric capacitive structures.

## II. Stabilized EFIE on Capacitive Problem

### A. Convergence of Conventional EFIE on Capacitive Problem

The EFIE operator can be written in its mixed potential form with two terms, the smooth term ($\mathcal{T}_s$) and the hypersingular term ($\mathcal{T}_h$) as

$$\mathcal{T}(\mathbf{J}) = \mathcal{T}_s(\mathbf{J}) + \mathcal{T}_h(\mathbf{J}) \tag{1}$$

$$\mathcal{T}_s(\mathbf{J}) = i\omega\mu\hat{\mathbf{n}}_{\mathbf{r}} \times \int_\Gamma g(\mathbf{r},\mathbf{r}')\mathbf{J}(\mathbf{r}')d\mathbf{r}' \tag{2}$$

$$\mathcal{T}_h(\mathbf{J}) = -\frac{1}{i\omega\epsilon}\hat{\mathbf{n}}_{\mathbf{r}} \times \nabla \int_\Gamma g(\mathbf{r},\mathbf{r}')\nabla' \cdot \mathbf{J}(\mathbf{r}')d\mathbf{r}' \tag{3}$$

where $g$ denotes the free-space Green's function, $\epsilon$ and $\mu$ are the relative permeability and permittivity, respectively, and $\mathbf{J}$ is the unknown current of a surface whose unit normal pointing outward at $\mathbf{r}$ is $\hat{\mathbf{n}}_{\mathbf{r}}$.

It is well known that the EFIE operator has a low-frequency breakdown problem due to the null space of the divergence operator. The hypersingular term, which is also known as the charge term, dominates when the frequency goes to zero. Thus, the null space in this integral operator results in an ill-conditioned matrix, where the eigenvalues of the system can be very large, corresponding to the irrotational current when the charge term dominates, and very small, corresponding to the solenoidal current when the induction term dominates. However, the solenoidal currents along the capacitive surfaces are trivial because of the open-circuited gap. This implies that the eigenvectors with very small eigenvalues cannot be excited with the delta-gap excitation. Therefore, the EFIE operator remains stable at very low frequencies for a capacitive problem. Generally speaking, this is mainly because the dominant charge term corresponding to the electroquasistatic equations captures the circuits physics for capacitors, and the swamped induction term is trivial in describing the capacitive problem.

As a numerical example, we consider a parallel-plate capacitor with the physical size of 4 mm × 5 mm × 0.4 mm. The number of unknowns is 553 with 394 triangular patches. The distributions of the eigenvalues for resultant matrices are plotted in the complex plane, as shown in Fig. 1. As for the case of traditional EFIE, at a very low frequency (1 Hz), the overall distribution is dispersive in a wide range. By applying a simple diagonal preconditioner (DP), the eigenvalue spectrum is compressed. From the perspective of the frequency, there are values accumulating around zero at both very low frequencies (1 Hz) and relatively higher frequencies (1 GHz) for both EFIE and EFIE with DP. It should be noted that both 1 Hz and 1 GHz are within the low-frequency range since the physical size of the model is from the scale of $10^{-11}\lambda$ to $10^{-2}\lambda$. ($\lambda$ is the wavelength in free space. For "low frequency," we were talking about the situations when the object size is much less than the wavelength, usually less than $\lambda/20$.) The spectrum properties should imply that the systems are ill-posed. However, when taking a look at the detailed convergence information as shown in Table I for EFIE with DP, we find that the iterative system remains stable at very low frequencies with accurate capacitance being achieved (compare with [20]). Also, the condition number is very large at very low frequencies due to some very small eigenvalues. When the frequency becomes higher, the condition number becomes smaller; however, convergence becomes worse, and the spectral radius $\rho$ almost remains the same. It implies that the values of small eigenvalues becomes higher with the frequency increasing. The fact that $\rho > 1$ implies that the convergence of system cannot be guaranteed. A similar conclusion can be drawn for the case of dense meshes with 2288 unknowns. The system matrix becomes even more ill conditioned, and the convergence becomes very slow as the mesh density increases.

TABLE I
CAPACITANCE AND CONVERGENCE INFORMATION OF THE MOM MATRIX UNDER EFIE WITH DP. TOLERANCE ERROR $= 10^{-4}$

| | EFIE, $N = 553$, $N_\sigma^{small} = 160$ | | | | EFIE, $N = 2288$, $N_\sigma^{small} = 713$ | | | static EFIE, $N = 553$ | | |
|---|---|---|---|---|---|---|---|---|---|---|
| $f$ (GHz) | $C$ (pF) | No. iter. | Cond. | $\rho = \max\|\lambda_i\|$ | No. iter. | Cond. | $C$ (pF) | No. iter. | Cond. | $C$ (pF) |
| $10^{-20}$ | 0.4723 | 36 | $3.7 \times 10^{18}$ | 1.9895 | 86 | $2.0 \times 10^{19}$ | 0.4769 | 36 | $3.8 \times 10^{18}$ | 0.4723 |
| $10^{-9}$ | 0.4723 | 36 | $6.4 \times 10^{19}$ | 1.9895 | 86 | $3.5 \times 10^{20}$ | 0.4769 | 36 | $6.4 \times 10^{19}$ | 0.4723 |
| $10^{-2}$ | 0.4723 | 36 | $1.5 \times 10^{9}$ | 1.9895 | 86 | $8.5 \times 10^{9}$ | 0.4769 | 36 | $4.5 \times 10^{17}$ | 0.4723 |
| $10^{-1}$ | 0.4724 | 36 | $1.5 \times 10^{7}$ | 1.9895 | 86 | $8.5 \times 10^{7}$ | 0.4769 | 36 | $3.9 \times 10^{17}$ | 0.4723 |
| 1 | 0.4766 | 272 | $1.5 \times 10^{5}$ | 1.9899 | 40650 | $8.5 \times 10^{5}$ | 0.4812 | 36 | $3.5 \times 10^{17}$ | 0.4723 |
| 5 | 0.6137 | 2505 | $6.1 \times 10^{3}$ | 1.9899 | 22797 | $3.4 \times 10^{4}$ | 0.6141 | 36 | $3.2 \times 10^{17}$ | 0.4709 |

$N$: the number of unknowns; $N_\sigma^{small}$: the number of small singular values.

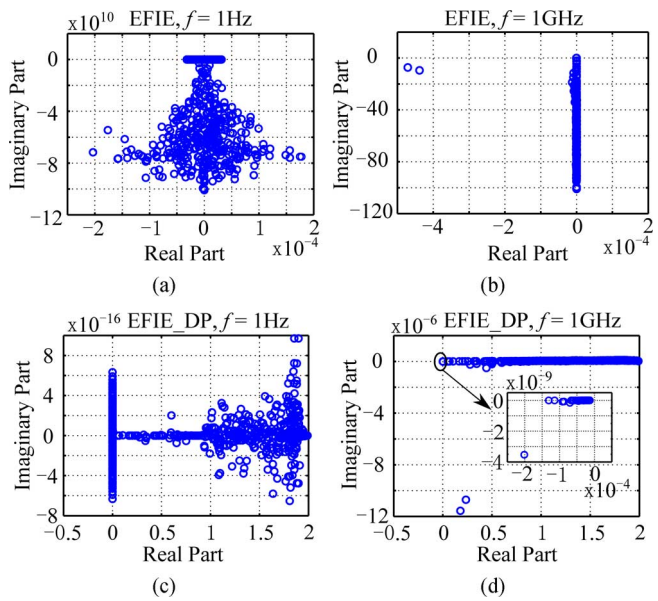


Fig. 1. Eigenvalues distribution of the MoM matrix under EFIE and EFIE with DP: (a) EFIE at 1 Hz; (b) EFIE at 1 GHz; (c) EFIE_DP at 1 Hz; and (d) EFIE_DP at 1 GHz.

### *B. Mathematical Manipulations of System Convergence With RHS Effect*

In the above case, we find that it is hard to explain the convergence phenomenon either using condition number or eigenvalue spectrum properties. Actually, eigenvalue spectrum and condition number are the properties of the impedance matrix, which is on the left-hand side of the system equation. Typically, the convergence of an iterative solver also depends on the right-hand side of the equation, which corresponds to the nature of the exciting source that generates the incident field [3]. The effect of the right-hand side can be described by performing the SVD analysis of a typical system

$$\bar{\mathbf{A}} \cdot \mathbf{x} = \mathbf{b}. \tag{4}$$

The singular value decomposition of the matrix $\bar{\mathbf{A}}$ is

$$\bar{\mathbf{A}} = \bar{\mathbf{U}}\bar{\Sigma}\bar{\mathbf{V}}^T. \tag{5}$$

We denote the singular vectors in $\bar{\mathbf{V}}$ to be $\mathbf{v}_n$, which are orthogonal to each other, and assume that the unknown vector can be written as

$$\mathbf{x} = \sum_{n=1}^{N} c_n \mathbf{v}_n \tag{6}$$

where $N$ denotes the dimension of the problem, and $c_n$ is a series of coefficients. By substituting (6) into (4) and testing the equation with $\mathbf{u}_m$ which are the singular vectors in $\bar{\mathbf{U}}$, the coefficients $c_m$ can be deduced as

$$c_m = \frac{\langle \mathbf{u}_m, \mathbf{b} \rangle}{\langle \mathbf{u}_m, \mathbf{u}_m \rangle \sigma_m} \tag{7}$$

where $\sigma_m$ is the $m$th singular value. So the contribution of the singular vectors in a solution depends very much on the singular values as well as the right-hand side, which will excite different modes. Each mode corresponds to a singular vector that can be treated as a basis current. The convergence becomes poor if the modes with small singular values are excited. Hence, we can calculate the contribution from different modes with the coefficients $c_n$.

For a more mathematical representation, the convergence phenomenon can be interpreted based on the Krylov subspace method. The Krylov subspace $\mathcal{K}^K(\bar{\mathbf{A}}, \mathbf{r}_0)$ is defined as

$$\mathcal{K}^K(\bar{\mathbf{A}}, \mathbf{r}_0) = \text{span}\{\mathbf{r}_0, \bar{\mathbf{A}} \cdot \mathbf{r}_0, \bar{\mathbf{A}}^2 \cdot \mathbf{r}_0, \ldots, \bar{\mathbf{A}}^K \cdot \mathbf{r}_0\} \tag{8}$$

where $\mathbf{r}_0 = \mathbf{b} - \bar{\mathbf{A}} \cdot \mathbf{x}_0$ is the initial residual error, and $\mathbf{x}_0$ is the initial estimate of the solution. The best estimate solution has the residual error in the $K$th iteration as

$$\mathbf{r}_K = \sum_{k=0}^{K} a_k \bar{\mathbf{A}}^k \cdot \mathbf{r}_0 = P_K^0(\bar{\mathbf{A}}) \cdot \mathbf{r}_0. \tag{9}$$

Here, $P_K^0(\bar{\mathbf{A}})$ is a $K$th-order polynomial of the matrix $\bar{\mathbf{A}}$ with $P_K^0(0) = 1$. Different iterative solvers aims at finding the coefficients $a_k$'s using different strategies through some threshold constrains.

To understand how the convergence issue relates to the right-hand side, one can re-derive the typical Krylov subspace method analysis as follows by presenting the right-hand side explicitly.

For a symmetric matrix $\bar{\mathbf{A}}$, $\mathbf{r}_0$ can be expanded in terms of the left and right singular vectors of $\bar{\mathbf{A}}$,

$$\mathbf{r}_0 = \sum_{n=1}^{N} \mathbf{v}_n \langle \mathbf{u}_n, \mathbf{r}_0 \rangle. \tag{10}$$

Then the $K$th term of (9) becomes

$$\begin{aligned} \bar{\mathbf{A}}^k \cdot \mathbf{r}_0 &= \bar{\mathbf{A}}^k \cdot \sum_{n=1}^{N} \mathbf{v}_n \langle \mathbf{u}_n, \mathbf{r}_0 \rangle \\ &= \sum_{n=1}^{N} \sigma_n^k \mathbf{u}_n \langle \mathbf{u}_n, (\mathbf{b} - \bar{\mathbf{A}} \cdot \mathbf{x}_0) \rangle \\ &= \sum_{n=1}^{N} \sigma_n^k \mathbf{u}_n \{ \langle \mathbf{u}_n, \mathbf{b} \rangle - \langle \mathbf{u}_n, \bar{\mathbf{A}} \cdot \mathbf{x}_0 \rangle \}. \end{aligned} \tag{11}$$

Note that $\bar{\mathbf{U}}^T \cdot \bar{\mathbf{A}} = \bar{\Sigma} \cdot \bar{\mathbf{V}}^T$ and from (7), the above equation can be reduced to

$$\bar{\mathbf{A}}^k \cdot \mathbf{r}_0 = \sum_{n=1}^{N} \sigma_n^k S_n \mathbf{u}_n \tag{12}$$

where $S_n = \sigma_n (c_n - \langle \mathbf{v}_n, \mathbf{x}_0 \rangle)$. Here, $S_n$ describes the contribution of the right-hand side and the initial estimated solution in the iterative process. Thus, it indicates that the contribution of singular vectors in the iterative process depends on not only the their corresponding singular values but also the coefficients $c_n$, which contain the information from both the matrix and the right-hand side.

More explicitly, the residual error in the $K$th iteration can be written as

$$\begin{aligned} \mathbf{r}_K &= \sum_{k=0}^{K} a_k \bar{\mathbf{A}}^k \cdot \mathbf{r}_0 = \sum_{k=0}^{K} a_k \sum_{n=1}^{N} \sigma_n^k S_n \mathbf{u}_n \\ &= \sum_{n=1}^{N} \left( \sum_{k=0}^{K} a_k \sigma_n^k \right) S_n \mathbf{u}_n \\ &= \sum_{n=1}^{N} P_K^0(\sigma_n) S_n \mathbf{u}_n. \end{aligned} \tag{13}$$

Here, we take GMRES iterative method as an example to provide the upper bound of the convergence rate. In this case, we need to seek the minimum of $\|\mathbf{r}_K\|$ subject to $\mathbf{z}_K = \mathbf{x}_K - \mathbf{x}_0 \in \mathcal{K}^K(\bar{\mathbf{A}}, \mathbf{r}_0)$ as

$$\begin{aligned} \min_{\mathbf{z}_K \in \mathcal{K}^K(\bar{\mathbf{A}}, \mathbf{r}_0)} \|\mathbf{r}_K\| &= \min_{P_K^0(x)} \left\| \sum_{n=1}^{N} P_K^0(\sigma_n) S_n \mathbf{u}_n \right\| \\ &\le \min_{P_K^0(x)} \sum_{n=1}^{N} |P_K^0(\sigma_n)| \, |S_n| \, \|\mathbf{u}_n\| \\ &= \sum_{n=1}^{N} \min_{P_K^0(x)} |P_K^0(\sigma_n)| \, |S_n| \, \|\mathbf{u}_n\|. \end{aligned} \tag{14}$$

All that is needed is an upper bound of the scalar function $\min_{P_k^0(x)} |P_K^0(\sigma_n)|$. Referring to [22], similar convergence analysis can be done using real Chebyshev polynomials since all singular values $\sigma_n$ are real positive. The derivation begins with

$$\min_{P_K^0(x)} |P_K^0(\sigma_n)| \le \min_{P_k^0(x)} \max_{\sigma \in [\sigma_N, \sigma_1]} |P_K^0(\sigma)|. \tag{15}$$

The minimum of the right-hand side of the inequality can be reached by the polynomial

$$\hat{C}_K(\sigma) \equiv \frac{C_K\left(1 + 2\frac{\sigma - \sigma_1}{\sigma_1 - \sigma_N}\right)}{C_K\left(1 + 2\frac{-\sigma_1}{\sigma_1 - \sigma_N}\right)} \tag{16}$$

where $C_K(t)$ is the Chebyshev polynomial of the first kind of degree $K$ as defined by

$$C_K(t) = \begin{cases} \cos[K \cos^{-1}(t)], & -1 \le t \le 1 \\ \cosh[K \cosh^{-1}(t)], & |t| \ge 1. \end{cases} \tag{17}$$

As in the definition, the maximum of $C_K$ for $t$ in $[-1, 1]$ is 1. Thus, we have

$$\min_{P_k^0(x)} \max_{\sigma \in [\sigma_N, \sigma_1]} |P_K^0(\sigma)| = \frac{1}{\left| C_K\left(1 + 2\frac{-\sigma_1}{\sigma_1 - \sigma_N}\right) \right|}. \tag{18}$$

Then, the upper bound of $\|\mathbf{r}_K\|$ can be obtained as

$$\min_{\mathbf{z}_K \in \mathcal{K}^K(\bar{\mathbf{A}}, \mathbf{r}_0)} \|\mathbf{r}_K\| = \frac{1}{\left| C_K\left(1 + 2\frac{-\sigma_1}{\sigma_1 - \sigma_N}\right) \right|} \sum_{n=1}^{N} |S_n| \, \|\mathbf{u}_n\| \tag{19}$$

which is codetermined by information from both the left-hand and right-hand side of the matrix equation. For a heuristic description, we can use the upper bound of the residual error to explain why the convergence of EFIE becomes slower when the frequency gets higher. Taking the parallel-capacitor as an example and referring to Fig. 2, the singular values suddenly drop to very small values at a point for both systems at 1 Hz and 1 GHz. The small singular values correspond to the null space, which will slow down the convergence. An iterative system is judged to be convergent if the residual error reached the manually set tolerance. We can calculate the contributions of modes for regular singular values ($\mathbf{r}_{\text{regular }\sigma}$) and small singular values ($\mathbf{r}_{\text{small }\sigma}$) in the residual error according to (19), respectively.

$$\begin{aligned} &\mathbf{r}_{\text{regular }\sigma} \propto 10^{-2}, \ \ \mathbf{r}_{\text{small }\sigma} \propto 10^{-14}, \ \ f = 1 \text{ Hz} \\ &\mathbf{r}_{\text{regular }\sigma} \propto 10^{-2}, \ \ \mathbf{r}_{\text{small }\sigma} \propto 10^{-5}, \ \ f = 1 \text{ GHz}. \end{aligned} \tag{20}$$

If the convergence threshold is set to be $10^{-3}$, then the contribution to the residual error from the small singular value modes are trivial for both cases. The combination of the regular singular values modes can meet the threshold requirements. However, usually the systems have not converged to accurate solutions at such a threshold. Or if higher accuracy is required, the threshold should be made lower. If it is chosen to be lower than $10^{-4}$, the contribution from the small singular value modes at 1 GHz becomes not negligible in affecting the convergence procedure, thus, leading to a worse convergence. On the contrary, as with the case of 1 Hz, the contribution from the small singular value modes is much smaller compared with the normal

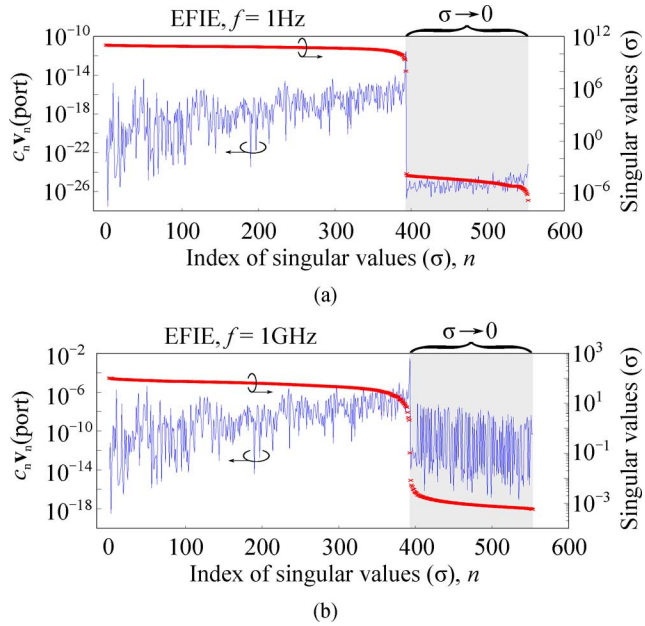


Fig. 2. Weights of contributions from singular vectors of EFIE in the port current after SVD: (a) at 1 Hz and (b) at 1 GHz.

convergence threshold we usually set, which is trivial in the iteration procedure.

### C. Right-Hand-Side Effect on Capacitive Problems

From the above section, we have known that the weights of the contribution from different modes can be obtained by calculating the coefficients $c_n$. Now looking back, the physical problem defined previously, as shown in Fig. 2 for the EFIE system, the decomposition of the currents at the port of the parallel-plate capacitor can be derived, where the singular values follow the descending order with respect to the index. It is important to note that the contribution from small singular value modes is trivial at 1 Hz. As the frequency increases, the influence of small singular-value modes becomes comparable to that of regular ones. It implies that the small singular value modes are not excited at very low frequencies. Physically speaking, the large singular value modes represent the irrotational current when the charge term (hypersingular term $\mathcal{T}_h$) dominates, while the small singular value modes correspond to the solenoidal current when the induction term (smooth term $\mathcal{T}_s$) dominates.

As depicted in Table I, the number of the small singular values ($N_\sigma^{\text{small}}$) is 160 in this numerical example. In other words, the number of the large singular values ($N_\sigma^{\text{large}}$) is 393, which is just equal to the number of charge currents

$$N_{\text{chargecurrents}} = N_{\text{patch}} - 1 = 393. \tag{21}$$

Thus, it means that the contribution from the charge currents is enough to describe the total current. Even though there is a null space, the system can still converge fast. However, the contribution from the induction term cannot be ignored any more when frequency increases, leading to a poor convergence of iterative process.

The EFIE system will break down at low frequencies and cannot capture the real physics if the smooth term is swamped. However, as discussed above, the smooth term is trivial when dealing with the capacitive problem. At the static limit ($\omega = 0$), the EFIE operator becomes

$$\mathcal{T}^{\text{static}} = \lim_{\omega\to 0}(\mathcal{T}_s + \mathcal{T}_h) \cong \mathcal{T}_h. \tag{22}$$

In fact, the solution solved from the static EFIE is a zeroth-order approximation of the entire solution. At low frequencies, the rest of the EFIE operator is a compact perturbation of the static counterparts since the kernel of the operator can be expanded as

$$\frac{e^{-jkR}}{R} = \frac{1}{R} + jk\cdot 1 + (jk)^2 R + \cdots = \frac{1}{R} + O(\omega^1). \tag{23}$$

Then, we can expect the small singular values of static EFIE operator to approach zero with the order of $\omega^1$. As shown in the last column of Table I, instead of poor convergence at higher frequencies for the original EFIE, the static EFIE remains stable over a wide frequency range. Similar explanation can be obtained by the analysis of the weights from different modes. As shown in Fig. 3, the distribution of the weights of the singular vectors in the port current for the static EFIE is similar to that of traditional EFIE at 1 Hz. However, when the frequency is increased to 1 GHz, similar to the behavior at 1 Hz, the contributions from those small singular value modes are trivial in the entire solution. Thus, the system can remain stable over a wide range of frequency, and it can be verified from the figure that the small singular values go to zero as $O(\omega^1)$. Also, as we know, EFIE has an approximate null space when $\omega \to 0$. When the frequency gets higher (not reaching middle frequency), the null space becomes less exact than that at very low frequencies. This results to the induction term showing up, which leads to the excitation of the singular vectors with small singular values. One may think that there is a tiny inductive effect here, which may excite the modes relates to the loop current. However, the capacitive property is still dominant. As with the static EFIE, which has an exact null space, the corresponding null space singular values should be exactly zero. Then, the nonzero null space singular values in Fig. 3 are due to numerical roundoff, numerical noise, or approximation. However, the approximation of the static EFIE extracting the capacitive physics may lose some accuracy in capturing the emerging inductive physics.

## III. Stabilized CMP-EFIE on Capacitive Problem

We can take the Calderón multiplicative preconditioned EFIE (CMP-EFIE) method as another example to present the right-hand-side effect. As mentioned above, CMP-EFIE is an effective remedy for the EFIE low-frequency breakdown. By applying the Calderón identity on EFIE, the EFIE operator "preconditions" itself, and the new operator becomes a well-conditioned second-kind integral operator. However, at very low frequencies, the CMP-EFIE method suffers from an inaccuracy problem for both closed surfaces and open capacitive problems [18], [20]. In [21], a simplified form of CMP-EFIE is claimed to be a stable and accurate formulation for capacitive problems at low frequencies. Here, the simplified CMP-EFIE is studied with the right-hand-side effect analysis. It is shown that the simplified formulation can achieve a current result of good accuracy at very low frequencies.

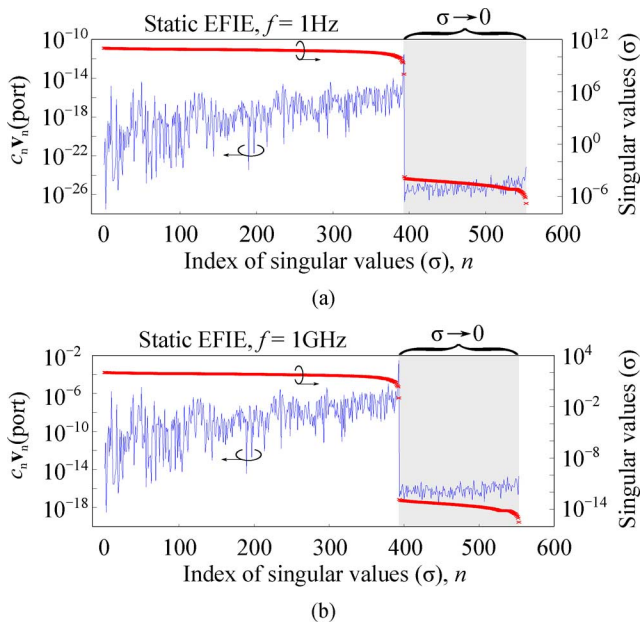


Fig. 3. Weights of contributions from singular vectors of static EFIE in the port current after SVD: (a) at 1 Hz and (b) at 1 GHz.

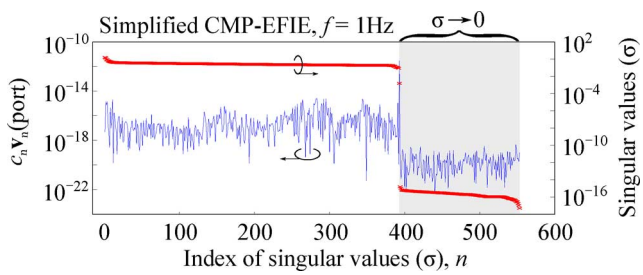


Fig. 4. Weights of contributions from singular vectors for the simplified CMP-EFIE. The frequency is 1 Hz.

### *A. Simplified CMP-EFIE for Low-Frequency Capacitive Problem*

Notice that CMP-EFIE formulation can be written as a combination of two constraints [21], the smooth preconditioned term

$$\mathcal{T}_s \cdot (\mathcal{T}_s + \mathcal{T}_h)(\mathbf{J}) = \mathcal{T}_s \cdot \mathbf{b}, \tag{24}$$

and the hypersingular preconditioned term

$$\mathcal{T}_h \cdot (\mathcal{T}_s + \mathcal{T}_h)(\mathbf{J}) = \mathcal{T}_h \cdot \mathbf{b}. \tag{25}$$

In [21], the hypersingular preconditioned term in (25) is proven to be trivial in describing the capacitive problem. Therefore, (24) can be treated as a simplified form of CMP-EFIE. From the formulation, it is actually a $\mathcal{T}_s$-preconditioned EFIE. As evidence, Fig. 4 presents the right-hand-side effect by showing the weight of contributions from singular vectors for (24). From physics, similar to EFIE, the new formulation of CMP-EFIE also remains stable at low frequencies because the contribution from the small singular vectors is trivial. And the resultant current can also be verified to be irrotational since the solenoidal basis vectors have little contribution to the total current. Furthermore, the accuracy of the current can be ensured at low frequencies under the formulation of (24), which will be further explained in the next subsection using the perturbation method.

### *B. Spectral Analysis With Perturbation Method*

As proposed in [18], [20], the perturbation method is used to remedy the inaccuracy problem in the CMP-EFIE. Here, the inaccuracy problem with capacitive structure is briefly reviewed.

The three-term decomposition of CMP-EFIE is unconditionally stable at low frequencies after manually setting $\mathcal{T}_h\mathcal{T}_h = 0$. From circuit physics analysis, we consider a lossless capacitor charged by a constant voltage $V$. Then, the current is given by $I = V/(1/j\omega C)$, from which we can conclude that $Im(I) \sim O(\omega)$. On the other hand, according to (23), the frequency dependence of the Green's function is $g \sim O(\omega^0, \omega^1)$. For the delta-gap excitation, the right-hand side is $\mathbf{V} \sim O(\omega^0, 0)$. Since the current basis function and the testing function is frequency invariant, the frequency dependence of the matrix equation can be obtained as

$$[\bar{\mathbf{Z}}^{ss}(\omega^2, \omega^3) + \bar{\mathbf{Z}}^{hs}(\omega^0, \omega^1) + \bar{\mathbf{Z}}^{sh}(\omega^0, \omega^1)] \cdot \mathbf{I}(\omega^a, \omega^b) = \bar{\mathbf{Z}}^{s}\mathbf{V}(0, \omega^1) + \bar{\mathbf{Z}}^{h}\mathbf{V}(0, \omega^{-1}). \tag{26}$$

Matching the frequency order of the two sides of the equation yields

$$b \geq -1. \tag{27}$$

For a capacitor, the imaginary part of current solved by the CMP-EFIE equation is of the order $\omega^{-1}$. It implies that the accurate current of a capacitor is a high-order subset of that from the CMP-EFIE formulation at low frequencies. Therefore, due to the finite computation precision, it is difficult to obtain the accurate imaginary part of the current, which is very important for circuits problems. However, doing the same thing for the simplified CMP-EFIE (24), the matching result corresponding to (26) should be $b \geq 1$, which indicates that the solved current is of the correct order of the frequency. This ensures the accuracy of the simplified system. In the following, we will use the perturbation method to analyze and verify our conclusion.

With the perturbation method, impedance matrices, current unknowns, and excitation vectors can all be expanded with respect to a small parameter $\delta = ik_0$. Obviously, all the matrices and vectors in the equations become frequency invariant. Matching the coefficients of like powers of $\delta$, the solution of current $\mathbf{j}$ can be obtained at different frequency orders, respectively. Since the unknowns are $ik_0\mathbf{j}$ in the formulation of CMP-EFIE with perturbation, only the equation corresponding to the second order of current needs to be solved for capacitive problems

$$[\bar{\mathbf{Z}}^{s(0)}_{CWBC}\bar{\mathbf{G}}_m^{-1}\bar{\mathbf{Z}}^{h(0)}_{RWG} + \bar{\mathbf{Z}}^{h(0)}_{CWBC}\bar{\mathbf{G}}_m^{-1}\bar{\mathbf{Z}}^{s(0)}_{RWG}] \cdot \mathbf{j}^{(2)} = [\bar{\mathbf{Z}}^{s(0)}_{CWBC}\bar{\mathbf{G}}_m^{-1} + \bar{\mathbf{Z}}^{h(2)}_{CWBC}\bar{\mathbf{G}}_m^{-1}] \cdot \mathbf{b}^{(0)} \tag{28}$$

where higher order currents have been ignored since they are much smaller at low frequencies. Similar to that in Section III-A, we can simply remove the smooth term from (28), which denotes induction physics. Furthermore, from the

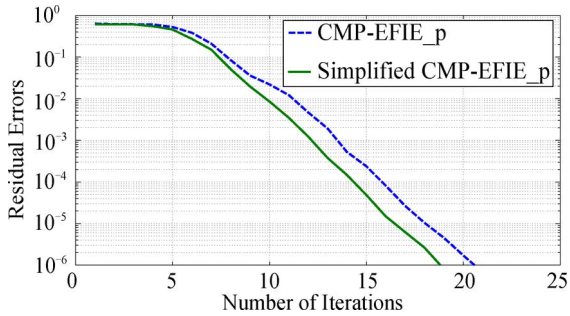


Fig. 5. Comparison of iteration number of original and simplified CMP-EFIE with perturbation method. The frequency is 1 Hz.

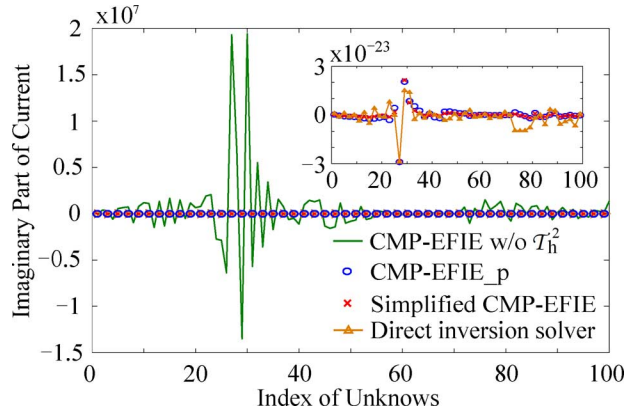


Fig. 6. Comparison of the imaginary current using the simplified CMP-EFIE, the CMP-EFIE with and without the perturbation method, and the direct inversion method of the CMP-EFIE with perturbation. The frequency is $10^{-11}$ Hz.

analysis in Section III-A, since (25) is trivial in describing the capacitor problem, then it can be concluded that the term $\mathcal{T}_h \cdot \mathbf{b}$ is trivial in the right-hand side. Thus, the term $\bar{\mathbf{Z}}^{h(2)}_{CWBC} \cdot \bar{\mathbf{G}}_m^{-1} \cdot \mathbf{b}^{(0)}$ should equal to zero in (28). Thus, we can rewrite (28) as

$$\bar{\mathbf{Z}}^{s(0)}_{CWBC} \cdot \bar{\mathbf{G}}_m^{-1} \cdot \bar{\mathbf{Z}}^{h(0)}_{RWG} \cdot \mathbf{j}^{(2)} = \bar{\mathbf{Z}}^{s(0)}_{CWBC} \cdot \bar{\mathbf{G}}_m^{-1} \cdot \mathbf{b}^{(0)}. \quad (29)$$

It is interesting to note that it becomes the static EFIE formulation with a smooth term as preconditioner. As shown in Fig. 5, the simplified form in (29) remains stable and converges even faster than the original one in (28). As also shown in (24), the term $\mathcal{T}_s\mathcal{T}_s$ is a compact counterpart. Hence, (24) also yields the form of (29) at low frequencies. Fig. 6 plots the calculated imaginary currents of a parallel-plate capacitor by different methods at the frequency of $10^{-11}$ Hz. Obviously, large errors are involved in the current obtained from the three-term CMP-EFIE formulation. On the contrary, the simplified CMP-EFIE and CMP-EFIE with perturbation method can still achieve a good stability at such a low frequency. A comparison is also done with the direct inversion method of the CMP-EFIE with perturbation formulation, which would be a reliable reference. Shown in the top right corner of Fig. 6, an imaginary current solved from the simplified CMP-EFIE and the CMP-EFIE with the perturbation method can achieve a good agreement. In addition, they are of the same order of the results by using the direct inversion solver, which indicates that the accuracy of the simplified formulation is ensured. Moreover, as shown in Fig. 7, the simplified system in (29) converges much faster than the EFIE and EFIE with DP and can also remain stable at both of the two frequencies.

More information can be obtained from the influence of the right-hand side. Fig. 8 shows the weight of contributions from singular vectors for the original and simplified CMP-EFIE with perturbation formulation. Similar to the EFIE, the simplified system also has 160 singular values that approach to zero, which have trivial contribution to the current at the port. Interestingly, in the original system, they have equally important contributions on the singular values and the weight corresponding to the smallest singular value is relatively higher. (For CMP-EFIE, due to the preconditioner, the singular values are redistributed. The smallest singular value corresponds to the lowest order current mode, which is the dominant current component. That is why the dominant singular-value weight relates to the smallest singular value.) Therefore, the simplified

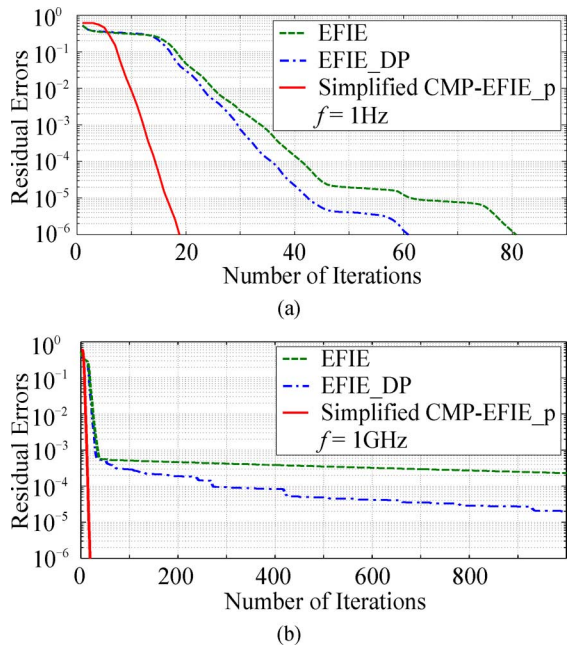


Fig. 7. Comparison of iteration number of EFIE, EFIE with DP and simplified CMP-EFIE with perturbation: (a) At 1 Hz and (b) At 1 GHz.

system converges even faster, because the contributions of singular vectors with small singular values are suppressed in comparison with the original one.

## IV. More Numerical Results With Parallel-Plate Capacitors

Both EFIE and CMP-EFIE converge well at low frequencies for capacitive problems. However, the convergence of EFIE is more sensitive to the number of unknowns. In Table II, we show the convergence for parallel-plate capacitors when the width of the parallel plate ($w$) is varying while its length is fixed as 5 mm. The frequency is 1 Hz, and the mesh size is chosen to be 0.25 mm ($(1/6) \times 10^{-11}\lambda$). $N$ is the number of unknowns. It shows that the convergence of both CMP-EFIE with perturbation and simplified CMP-EFIE with perturbation remains stable regardless of the increasing number of unknowns when the mesh size

TABLE II
COMPARISON OF CONVERGENCE USING THE METHOD OF EFIE (WITH DP), STATIC EFIE (WITH DP), CMP-EFIE WITH PERTURBATION AND SIMPLIFIED CMP-EFIE WITH PERTURBATION AT 1 HZ

| Methods | Number of Iteration (GMRES-30 and Tolerance: $1 \times 10^{-6}$) | | | |
|---|---|---|---|---|
| | $w$ = 1mm, $N$ = 480 | $w$ = 2mm, $N$ = 1054 | $w$ = 4mm, $N$ = 2082 | $w$ = 5mm, $N$ = 2626 |
| EFIE | 32 | 36 | 60 | 80 |
| Static EFIE | 32 | 36 | 60 | 80 |
| CMP-EFIE_p | 24 | 23 | 23 | 23 |
| Simplified CMP-EFIE_p | 22 | 20 | 20 | 21 |

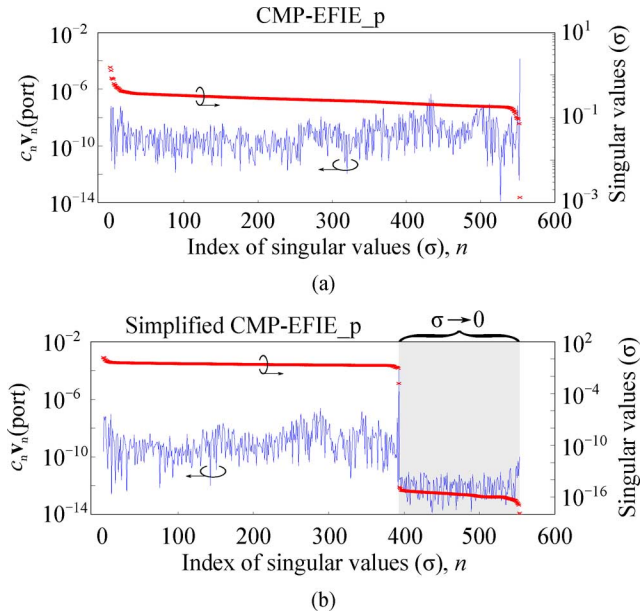


Fig. 8. Weights of contributions from singular vectors of CMP-EFIE with perturbation in the port current after SVD at 1 Hz: (a) original CMP-EFIE with perturbation and (b) simplified CMP-EFIE with perturbation.

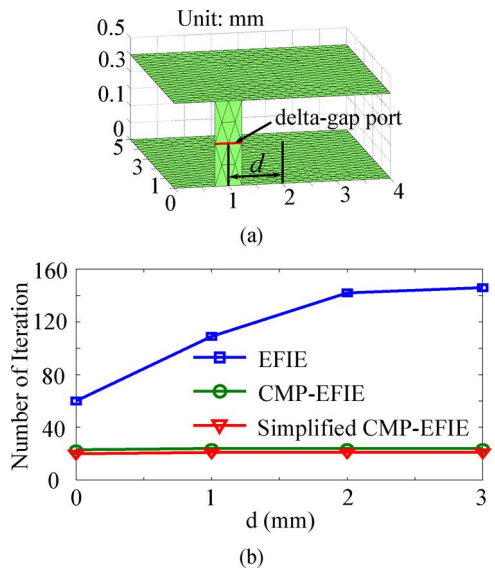


Fig. 9. (a) Geometry of parallel plate capacitor with asymmetric excitation position. (b) Comparison of the convergence with the position of the excitation using EFIE (with DP), static EFIE (with DP), CMP-EFIE with perturbation, and simplified CMP-EFIE with perturbation at 1 Hz.

is fixed. While the convergence of EFIE and static EFIE begin to slow down with the increase of the number of unknowns.

The instability of the formulation of EFIE dealing with capacitive problems also occurs when the structure is asymmetric. As shown in Fig. 9(a), the excitation point of the capacitor is moved away from the symmetric position, and Fig. 9(b) shows the convergence of EFIE, CMP-EFIE, and the simplified CMP-EFIE with the position of the excitation at 1 Hz. It implies that the results of CMP-EFIE and simplified CMP-EFIE is almost immune to the position of the excitation point, while the convergence of EFIE becomes worse and worse when the excitation point is moving away from the central position. The possible reason is that the asymmetric feeding excites some high-order modes, which can be annihilated by the smoothing property of a compact operator like three-term CMP-EFIE or simplified CMP-EFIE. However, the noncompact nature of the EFIE operator enhances the high-order components, and then the divergence behavior occurs.

## V. CONCLUSION

In this paper, the right-hand-side effect is taken into consideration to explain the convergence phenomenon of the EFIE-based systems. Regardless of the unimportant terms, the simplified and stabilized forms for the low-frequency EFIE and CMP-EFIE for open capacitors have been presented. Following the detailed right-hand-side effect analysis, the EFIE operator has been found to be stable and has fast convergence at very low frequencies. This is mainly because the charge current is enough to describe the total current of a capacitor, while the singular vectors with small singular values have not been excited with delta-gap excitation at low frequencies. Moreover, it has been shown that the smooth term can be employed to precondition the hypersingular term, where a stabilized and accurate form of CMP-EFIE at low frequencies has been achieved. With the perturbation method, it is easy to understand that the stabilized CMP-EFIE form is also the zeroth-order approximation at low frequencies, where higher order terms should be considered when the frequency is higher. More results have shown that EFIE is more sensitive than the CMP-EFIE to the right-hand-side excitation.

## ACKNOWLEDGMENT

S. Sun would like to thank Dr. Q. Dai, The University of Illinois at Urbana-Champaign, for his valuable discussion in this work.

## REFERENCES


[1] Y. Zhang, T. J. Cui, W. C. Chew, and J. S. Zhao, "Magnetic field integral equation at very low frequencies," *IEEE Trans. Antennas Propag.*, vol. 51, no. 8, pp. 1864–1871, Aug. 2003.

[2] K. Cools, F. P. Andriulli, D. D. Zutter, and E. Michielssen, "Accurate and conforming mixed discretization of the MFIE," *IEEE Antennas Wireless Propag. Lett.*, vol. 10, pp. 528–531, 2011.

[3] W. C. Chew, M. S. Tong, and B. Hu, *Integral Equation Methods for Electromageneic and Elatic Waves*. San Rafael, CA, USA: Morgan & Claypool, 2008.

[4] A. F. Peterson, C. F. Smith, and R. Mittra, "Eigenvalues of the moment-method matrix and their effect on the convergence of the conjugate gradient algorithm," *IEEE Trans. Antennas Propag.*, vol. 36, no. 8, pp. 1177–11179, Aug. 1988.

[5] R. J. Adams, "Physical and analytical properties of a stabilized electric field integral equation," *IEEE Trans. Antennas Propag.*, vol. 52, no. 2, pp. 362–372, Feb. 2004.

[6] J. S. Zhao and W. C. Chew, "Integral equation solution of Maxwell's equations from zero frequency to microwave frequency," *IEEE Trans. Antennas Propag.*, vol. 48, no. 10, pp. 1635–1645, Oct. 2000.

[7] D. R. Wilton and A. W. Glisson, "On improving the stability of the electric field integral equation at low frequencies," in *Proc. URSI Radio Sci. Meet.*, Los Angeles, CA, USA, Jun. 1981, p. 24.

[8] J. R. Mautz and R. F. Harrington, "An E-field solution for a conducting surface small or comparable to the wavelength," *IEEE Trans. Antennas Propag.*, vol. 32, no. 4, pp. 330–339, Apr. 1984.

[9] Z. G. Qian and W. C. Chew, "Fast full-wave surface integral equation solver for multiscale structure modeling," *IEEE Trans. Antennas Propag.*, vol. 57, no. 11, pp. 3594–3601, Nov. 2009.

[10] F. Vipiana, P. Pirinoli, and G. Vecchi, "Spectral propertie of the EFIE-MoM matrix for dense meshes with different type of bases," *IEEE Trans. Antennas Propag.*, vol. 55, no. 11, pp. 3229–3238, Nov. 2007.

[11] G. C. Hsiao and R. E. Kleinman, "Mathematical foundations for error estimation in numerical solutions of integral equations in electromagnetics," *IEEE Trans. Antennas Propag.*, vol. 45, no. 3, pp. 316–328, Mar. 1997.

[12] H. Contopanagos, B. Dembart, M. Epton, J. J. Ottusch, V. Rokhlin, J. L. Visher, and S. M. Wandzura, "Well-conditioned boundary integral equations for three-dimensional electromagnetic scattering," *IEEE Trans. Antennas Propag.*, vol. 50, no. 12, pp. 1824–1830, Dec. 2002.

[13] F. P. Andriulli, K. Cools, H. Bagci, F. Olyslager, A. Buffa, S. Christiansen, and E. Michielssen, "A multiplicative Calderón preconditioner for the electric field integral equation," *IEEE Trans. Antennas Propag.*, vol. 56, no. 8, pp. 2398–2412, Aug. 2008.

[14] M. B. Stephanson and J.-F. Lee, "Preconditioner electric field integral equation using Calderón identities and dual loop/star basis functions," *IEEE Trans. Antennas Propag.*, vol. 57, no. 4, pp. 1274–1279, Apr. 2009.

[15] S. Yan, J.-M. Jin, and Z. Nie, "EFIE analysis of low-frequency problems with loop-star decomposition and Calderón multiplicative preconditioner," *IEEE Trans. Antennas Propag.*, vol. 58, no. 3, pp. 857–867, Mar. 2010.

[16] F. P. Andriulli, K. Cools, I. Bogaert, and E. Michielssen, "On a well-conditioned electric field integral operator for multiply connected geometries," *IEEE Trans. Antennas Propag.*, vol. 61, no. 4, pp. 2077–2087, Apr. 2013.

[17] J. Peeters, I. Bogaert, K. Cools, J. Fostier, and D. D. Zutter, "Combining Calderón preconditioning with fast multiple methods," presented at the IEEE Int. Symp. Antennas Propag., Toronto, ON, Canada, Jul. 2010.

[18] S. Sun, Y. G. Liu, W. C. Chew, and Z. Ma, "Calderón multiplicativepreconditioned EFIE with perturbation method," *IEEE Trans. Antennas Propag.*, vol. 61, no. 1, pp. 247–255, Jan. 2013.

[19] Z. G. Qian and W. C. Chew, "Enhanced A-EFIE with perturbation method," *IEEE Trans. Antennas Propag.*, vol. 58, no. 10, pp. 3256–3264, Oct. 2010.

[20] Q. S. Liu, S. Sun, and W. C. Chew, "Low-frequency CMP-EFIE with perturbation method for open capacitive problems," presented at the IEEE Int. Symp. Antennas Propag., Chicago, IL, USA, Jul. 2012.

[21] Q. S. Liu, S. Sun, and W. C. Chew, "Implementation of a simplified form of CMP-EFIE for low-frequency capacitive problems," in *Proc. IEEE Int. Symp. Antennas Propag.*, Orlando, FL, USA, Jul. 2013, pp. 75–76.

[22] Y. Saad, *Iterative Methods for Sparse Linear Systems*, 2nd ed. Philadelphia, PA, USA: SIAM, 2003.


**Qin S. Liu** (S'12) received the B.Eng. degree in electronic engineering from the University of Science and Technology of China (USTC), Hefei, China, in 2011.

She is currently working towards the Ph.D. degree in electrical and electronic engineering in the University of Hong Kong, Hong Kong, China. Her research interests include numerical methods and fast algorithms in computational electromagnetics.

**Sheng Sun** (S'02–M'07–SM'12) received the B.Eng. degree in information engineering from the Xi'an Jiaotong University, China, in 2001 and the Ph.D. degree in electrical and electronic engineering from the Nanyang Technological University, Singapore, in 2006.

He was with the Institute of Microelectronics in Singapore from 2005 to 2006, and with the Nanyang Technological University, Singapore, from 2006 to 2008. He was a Humboldt Research Fellow with the Institute of Microwave Techniques at the University of Ulm, Germany, from 2008 to 2010. Since 2010, he has been a Research Assistant Professor with the Department of Electrical and Electronic Engineering at The University of Hong Kong. His research interests include electromagnetic theory and computational mathematics, multi-physics, numerical modeling of planar circuits and antennas, microwave passive and active devices, as well as the microwave and millimeter-wave communication systems. He has coauthored a book entitled *Microwave Bandpass Filters for Wideband Communications* and authored and coauthored over 100 journal and conference publications.

Dr. Sun received the ISAP Young Scientist Travel Grant, Japan, in 2004; the Hildegard Maier Research Fellowship of the Alexander Von Humboldt Foundation, Germany, in 2008; and the General Assembly Young Scientists Award from the International Union of Radio Science (URSI) in 2014. He also received the Outstanding Reviewer Award for the IEEE MICROWAVE AND WIRELESS COMPONENTS LETTERS in 2010. He has been an Associate Editor for the *IEICE Transactions on Electronics* since 2010.

**Weng Cho Chew** (S'79–M'80–SM'86–F'93) received the B.S. degree in 1976, both the M.S. and Engineer's degrees in 1978, and the Ph.D. degree in 1980, all in electrical engineering, from the Massachusetts Institute of Technology, Cambridge, MA, USA.

He worked on fast algorithms in computational electromagnetics in the last 20 years. From 1981 to 1985, he worked at Schlumberger–Doll Research as a Manager. In 1985, he joined the University of Illinois Urbana-Champaign (UIUC), Urbana, IL, USA, where he was the Director of the Electromagnetics Lab from 1995 to 2007. He was also the Founder Professor at UIUC from 2000 to 2005, and the Y. T. Lo Endowed Chair Professor from 2005 to 2009. From 2007 to 2011, he served as the Dean of Engineering at The University of Hong Kong. In 2006, he was a Cheng Tsang Man Professor at Nanyang Technological University (NTU), Singapore. He has authored and coauthored three books, over 350 journal papers, and over 400 conference papers. His research interests are in wave and field and multiphysics.

Dr. Chew is a fellow of the OSA, IOP, EM Academy, and HKIE. He is the winner of an IEEE Graduate Teaching Award, a Schekulnof Best Paper Award, and an IEEE Distinguished Lecturer Award. In 2006, he was a Cheng Tsang Man Professor at NTU, Singapore. In 2008, he received the CT Tai Distinguished Educator Award from IEEE AP-S. He has been the Editor-in-Chief of PIER journals since 2009. Recently, he has been elected as a member of the U.S. National Academy of Engineering. He is an ISI highly cited author.